Human Molecular Genetics, 2012, Vol. 21, No. 24 **5306–5317**
doi:10.1093/hmg/dds386
Advance Access published on September 13, 2012

Kinetochore KMN network gene CASC5 mutated in primary microcephaly

Anne Genin[1], Julie Desir[1,2], Nelle Lambert[1,2], Martine Biervliet[3], Nathalie Van Der Aa[3], Genevieve Pierquin[4], Audrey Killian[5], Mario Tosi[5], Montse Urbina[2], Anne Lefort[1], Frederick Libert[1], Isabelle Pirson[1,*] and Marc Abramowicz[1,2]

[1]Institute of Interdisciplinary Research IRIBHM and [2]Medical Genetics, Hôpital Erasme, Université Libre de Bruxelles, Anderlecht 1070, Belgium, [3]Department of Medical Genetics, University Hospital Antwerp, Antwerp 2000, Belgium, [4]Human Genetics, University of Liège, Liège 4000, Belgium and [5]Faculty of Medicine, Inserm U1079, IRIB, Rouen 76000, France,

Received May 30, 2012; Revised and Accepted September 7, 2012

Several genes expressed at the centrosome or spindle pole have been reported to underlie autosomal recessive primary microcephaly (MCPH), a neurodevelopmental disorder consisting of an important brain size reduction present since birth, associated with mild-to-moderate mental handicap and no other neurological feature nor associated malformation. Here, we report a mutation of *CASC5* (aka *Blinkin*, or *KNL1*, or *hSPC105*) in MCPH patients from three consanguineous families, in one of which we initially reported the MCPH4 locus. The combined logarithm of odds score of the three families was >6. All patients shared a very rare homozygous mutation of *CASC5*. The mutation induced skipping of exon 18 with subsequent frameshift and truncation of the predicted protein. CASC5 is part of the KMN network of the kinetochore and is required for proper microtubule attachment to the chromosome centromere and for spindle-assembly checkpoint (SAC) activation during mitosis. Like MCPH gene ASPM, CASC5 is upregulated in the ventricular zone (VZ) of the human fetal brain. CASC5 binds BUB1, BUBR1, ZWINT-1 and interestingly it binds to MIS12 through a protein domain which is truncated by the mutation. CASC5 localized at the equatorial plate like ZWINT-1 and BUBR1, while ASPM, CEP152 and PCTN localized at the spindle poles in our patients and in controls. Comparison of primate and rodent lineages indicates accelerated evolution of *CASC5* in the human lineage. Our data provide strong evidence for *CASC5* as a novel MCPH gene, and underscore the role of kinetochore integrity in proper volumetric development of the human brain.

INTRODUCTION

A large, convoluted brain is a hallmark of the *Homo sapiens* lineage, and is associated with human-specific skills, including the ability to orchestrate symbolic thought, language, tool use and emotional adaptation to the social environment. Conversely, a small brain, and particularly a small cerebral cortex, is a major feature of many developmental brain disorders (1).

The brain size correlates closely with the head circumference (HC). Microcephaly refers to a small HC in terms of standard deviations (SD) below the mean for age and gender. Primary microcephaly refers to a small brain size present since birth, with no structural malformation of the brain, with a HC < -2SD at birth and < -3SD after 1 year of age. From a theoretical standpoint, primary microcephaly may result from decreased cell proliferation during development, increased cell death or migration defects, these three groups of causes not excluding one another. Microcephaly, Primary Hereditary (MCPH) [MIM 251200] is an autosomal recessive trait with primary microcephaly, associated with mild-to-moderate mental handicap and absence of additional neurological or somatic disease. The brain may be very small, with an estimated volume hardly more than a third of the normal volume in some patients (2). MCPH is a very rare disorder in outbred populations, affecting $<1/100\,000$ newborns (3), but is more frequent in some populations with a high rate of consanguinity (4,5).

*To whom correspondence should be addressed at: 808, Route de Lennik, Anderlecht 1070, Belgium. Tel: +32 25554137; Email: ilpirson@ulb.ac.be

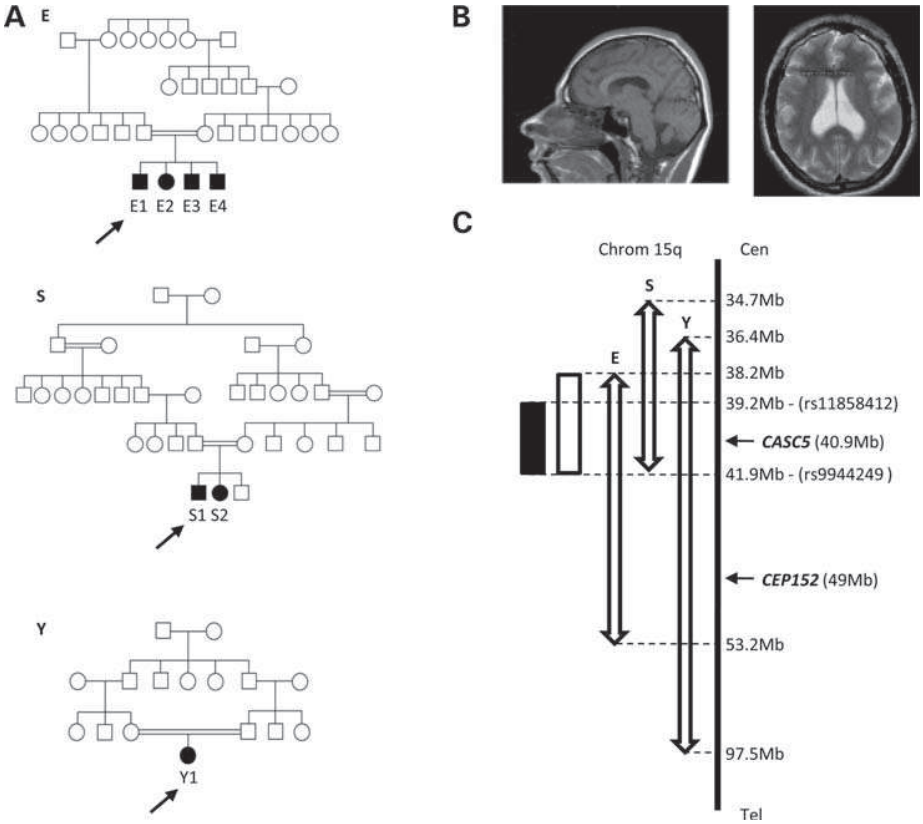

Figure 1. Linkage analysis. (**A**) E, S and Y are consanguineous families from three small villages in North-Eastern Morocco. Linkage to 15q (MCPH4) was previously reported in family E (18). (**B**) Brain MRI in proband E1 showing a small brain with shortened frontal lobes, simplified gyri and normal thickness of the cortex. Brain stem and cerebellum are of normal size for age. (**C**) Homozygosity mapping and linkage disequilibrium. Double-headed arrows indicate homozygous regions. The open box represents the 3.7 Mb critical region of overlapping linkage. The filled box represents the 2.7 Mb haplotype shared by the three families, with indication of the first non-shared single-nucleotide polymorphisms (SNPs) on both the sides. Both the boxes contain *CASC5* but not *CEP152* located at 40.9 Mb and 49 Mb, respectively, on chromosome 15q (hg19 assembly).

Because MCPH is Mendelian (single gene defect) and because microcephaly in general is a feature of many developmental brain disorders (1), MCPH is an illuminating model to dissect molecular mechanisms of brain development. MCPH is very heterogeneous, with ten loci and nine genes reported to date: *Microcephalin* (*MCPH1*, or *BRIT1*) (5), *WDR62* (MCPH2) (6), *CDK5RAP2* (MCPH3) (7), *CEP152* (MCPH4) (8), *ASPM* (MCPH5) (2), *CENPJ* (MCPH6) (7), *STIL* (MCPH7) (9), *CEP63* (10) and *CEP135* (11). In addition, an orphan locus has recently been reported at 10q (12). More genetic heterogeneity is to be expected considering the complexity of the process of human brain development. All nine genes reported to date encode proteins that localize to the centrosome (7,13,14) suggesting that a centrosomal mechanism is responsible for controlling the neural cell number in the developing human brain (7), with data supporting a role in regulating progenitors proliferation and cell cycle exit leading to neuronal differentiation (15,16). Another mechanism is, however, not excluded. MCPH1 has been involved in DNA repair (17).

In addition to genetic heterogeneity, some MCPH defects are allelic to complex syndromes that share microcephaly as a feature, e.g. lissencephaly with additional brain malformations (*WDR62*) (6), and Seckel syndrome (*CEP152* (8), *CENPJ* (7)).

We initially reported a relatively large (25 cM) MCPH linkage region on chromosome 15, MCPH4, after homozygosity mapping in a Moroccan family (18). In 2010, Guernsey *et al*. reported mutations of *CEP152* in unrelated MCPH patients, *CEP152* being located in our initial MCPH4 linkage region (8). Here, we report the mutation of a novel MCPH gene, *CASC5*, and the exclusion of *CEP152*, in our initial MCPH4 family and two previously unreported families.

RESULTS

Mapping and identification of a CASC5 homozygous mutation

The *ASPM* gene (the most frequently mutated gene in MCPH) was sequenced in each of the three families and no mutation was found. Genotyping the original MCPH4 family E, and families S and Y using 250 K GeneChip® microarrays showed a common region of homozygosity spanning 3.7 Mb at 15q14–15.1 (Fig. 1C, open box). This region was the only region in the whole genome that showed homozygosity

in the three families over a significant length consistent with autozygosity (>2 cM in each family). This 3.7 Mb segment clearly excluded the *CEP152* gene transcription unit, which is located 7 Mb outside of the linkage region. Furthermore, direct sequencing of all coding exons and intronic junctions of *CEP152* showed no mutation.

The three families originated from neighboring small villages in rural Morocco. Within the 3.7 Mb homozygous region, we observed a 2.7 Mb haplotype that was common to the three families, strongly suggesting linkage disequilibrium around an ancestral mutation (Fig. 1C).

This genomic region is rich in protein-coding genes, and the 2.7 Mb segment contains 38 genes. Two *in silico* methods to prioritize the best candidates were used: the Endeavour program and K_a/K_s analysis. The Endeavour program (www.esat.kuleuven.be/endeavour) aims at ranking a defined set of target genes (here, all genes of our 2.7 Mb segment) according to their expression, cellular function and other publicly available data after comparison with a defined set of educating genes. For the latter set, we used the known MCPH genes, as well as all genes known to be involved in centrosomal or spindle organization and function, and/or in the regulation of the mitotic cell cycle (Fig. 2A).

We computed the human/macaque and rat/mouse K_a/K_s for the range of our candidate genes in order to prioritize those with high ratios (Fig. 2B) (18).

We analyzed the patient's lymphoblasts transcriptome by the Affymetrix® gene expression array (Fig. 2C). We reasoned that a sizable, probably large fraction of mutations causing highly penetrant recessive phenotypes are complete loss-of-function mutations where premature stop codons cause nonsense-mediated mRNA decay. We focused on the genes contained in the critical interval, as well as on *CEP152*. *CASC5*, *EIF2AK4*, *FAM82C*, *CHAC1* and *THBS1* showed very low expression when compared with control in both probands for at least one of the probes, contrasting with *CEP152* which yielded a higher signal in the patients.

RAD51, *BUB1B*, *EIF2AK4*, *NUSAP1*, *PAK6*, *VPS18*, *ZFYVE19* and *CASC5* were sequenced by the Sanger method (Fig. 3A). Only one novel variant was discovered, a missense mutation in exon 18 of the *CASC5* gene. This homozygous-coding variant, c.6125 G>A, changed a methionine into an isoleucine residue at position 2041 of the protein (p. M2041I). Met2041 is highly conserved across species (Fig. 3B) and the substitution was scored as "probably damaging" by software PolyPhen2 (score of 0.996). Fifty-eight unrelated healthy controls of the same (Moroccan) ethnic origin and a 100 unrelated controls with mixed ethnicities were sequenced for this variant and all of them were negative (0 occurrence of the mutation in 316 alleles).

Under the assumption of a mutation frequency equal to 0.003, the combined logarithm of odds (LOD) score over the three families was >6.

The *CASC5* gene has 27 exons and codes for a protein which localizes at the kinetochore. The CASC5 protein performs two crucial functions during mitosis: it is required for correct attachment of chromosome centromeres to the microtubule apparatus, and is essential for spindle-assembly checkpoint (SAC) signaling (19). CASC5 directly links BUB1 and BUB1B to kinetochores (19). CASC5 also directly binds MIS12 which is essential for kinetochore formation and proper chromosome segregation during mitosis (20), and the interactions between NDC80, MIS12 and KNL1 (CASC5) are referred as the KMN network. The C-terminal portion of CASC5 (AA 1981–2108), containing the mutation, interacts with ZWINT-1, a kinetochore protein, required for kinetochore assembly and for proper SAC silencing at metaphase (Fig. 5A).

In order to rule out a disease-causing mutation in another gene, the full genomic 2.7 Mb critical region was captured on a customized microarray and sequenced using the 454 Roche FLX Genome Sequencer. Using a customized NimbleGen array with 60–90 nucleotide-long probes covering 74.3% of target bases, including 93.3% of protein-coding sequences and untranslated regions, we enriched DNA for the 2.7 Mb locus and sequenced the captured library. A total of 1 389 296 reads (445 659 360 bp) with an average length of 317 bp were sequenced. The length of the hybridized fragments being much larger than the capture probes, we were able to cover 97.5% of the target region. The depth of sequencing was >20-fold for 78% of the bases, >10-fold for 88% and >4-fold for 97%. After filtering the raw data for changes affecting less than two reads or <10% of the reads, we identified 1982 variants in the region, all homozygous as expected. One thousand seven hundred and nineteen were reported in single-nucleotide polymorphism (SNP) databases dbSNP128 and 263 were unknown. Variants were further filtered to remove polymorphisms present in dbSNP135. Two hundred and eight homozygous variants remained after filtering, consisting of 113 noncoding indels, and 94 noncoding single nucleotide variants (SNVs), in locations unlikely to have a functional effect (e.g. not located in first or last intronic dinucleotide). We identified a single coding, rare, unreported SNV, the c.6125 G>A mutation in *CASC5*. Of note, FLX sequencing also identified an unknown coding SNV in RTF1, but the latter was not confirmed by Sanger Sequencing (Table 1). A virtual *de novo* assembly of the FLX sequencing reads failed to detect a chimeric segment that would indicate a chromosomal rearrangement. In short, the only candidate mutation found in the 2.7 Mb fragment was the *CASC5* mutation (Fig. 3C).

Functional analysis of the mutation

The *CASC5* mutation was predicted to produce a semi-conservative amino acid change, transforming a methionine into an isoleucine residue, with a likely functional effect. More importantly, the mutation was predicted to inactivate an exonic splicing enhancer (ESE), as indicated by both the ESEfinder and RESCUE-ESE algorithms, leading to an abnormal transcript with an absent exon 18. Besides the important role of the exon 18-encoded protein domain (see discussion), skipping this exon produces a frameshift, with a premature stop codon in exon 19.

To demonstrate the abnormal splicing of the mutated *CASC5* in patients, RNA was extracted from lymphoblastoid cell lines, reverse transcribed into complementary DNA (cDNA) and amplified using primers targeting a 316 bp fragment encompassing exon 17 to exon 19 of *CASC5* (Fig. 4A). Two bands were observed after acrylamide gel electrophoresis. One band of normal size (316 bp) was present in all subjects. A smaller

A

Rank	Global Prioritization
1	VPS18
2	DISP2
3	NUSAP1
4	RAD51
5	FAM82C
6	ZFYVE19
7	NDUFAF1
8	PLCB2
9	D4ST1
10	OIP5
11	SPINT1
12	INOC1
13	IVD
14	CHAC1
15	C15orf23
16	ITPKA
17	BAHD1
18	BMF
19	BUB1B
20	RTF1
21	RPUSD2
22	PAK6
23	GPR176
24	THBS1
25	EXDL1
26	DNAJC17
27	SRP14
28	TYRO3
29	RPAP1
30	CASC5
31	RHOV
32	LTK
33	FSIP1
34	EIF2AK4
35	DLL4
36	CCDC32
37	GCHFR
38	PPP1R14D

B

Gene	Human vs Macaque	Mouse vs Rat	Primate/Rodent
MCPH1	0.6160	0.5406	1.1394
CDK5RAP2	0.6866	0.4073	1.6857
CENPJ	0.5430	0.3699	1.4679
ASPM	0.4940	0.3691	1.3383
RAD51	0.4338	0.4495	0.9650
NUSAP1	0.8070	0.4442	1.8167
CASC5	0.9398	0.5759	1.6318
FAM82C	0.2241	0.1364	1.6429
CHAC1	0.0856	0.1231	0.6953
VPS18	0.0187	0.0319	0.5862
ZFYVE19	1.0606	0.3290	3.2237
EIF2AK4	0.0792	0.1087	0.7286

C

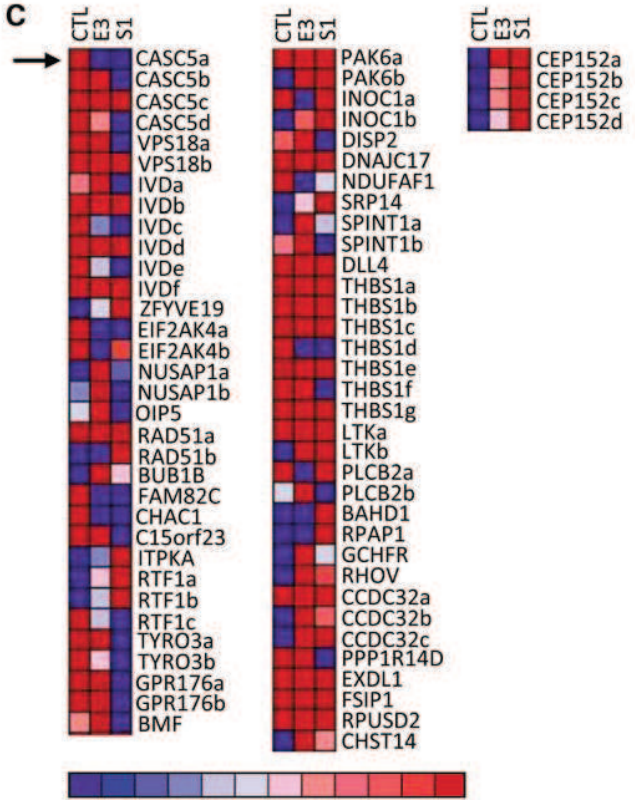

Figure 2. Prioritization of candidate genes. (**A**) Global ranking of our candidate genes using the Endeavor program, higher ranking indicating more likely candidate. (**B**) Computation of the K_a/K_s ratios in primates (human versus macaque, first column) and in rodents (mouse versus rat, second column). Higher ratios reflect more rapid evolution. The third column is the ratio between K_a/K_s in primates and rodents. A ratio of >1 indicates accelerated evolution of the gene in the *Homo Sapiens* lineage. MCPH1, CDK5RAP2, CENPJ and ASPM are known MCPH genes. (**C**) Transcriptome study. Heatmap generated using the GenePattern software, comparing expressions of all genes in the 2.7 Mb linkage interval, as well as CEP152, in control lymphoblasts and in lymphoblasts from patients E3 and S1. Red indicates the highest gene expression; dark blue indicates the lowest expression. Some transcripts are targeted by several probes indicated as a, b, c, d.

band of expected size (228 bp) for exon 18 deletion was observed only in the homozygous patient and heterozygous parents. This 228 bp smaller band seemed more intense in the patient's sample. Both the bands were extracted from the gel and sequenced, which confirmed that they consisted of exons 17-18-19, containing the variant c.6125 G>A and 17–19, respectively.

The impact of the mutation in abnormal *CASC5* splicing was further studied by a minigene experiment. The wild-type and mutant exon 18, flanked by 150 bp of intron sequences and inserted into the pCAS-1 minigene, was transfected into HeLa cells. Splicing products were visualized in agarose gels (Fig. 4B). An abnormal band of the expected size corresponding to the deletion of exon 18 was only observed from the mutated construct, confirming that the mutation was able to cause exon skipping *in vitro*.

CASC5 is a large protein of 265 KDa. The skipping of exon 18 is thus predicted to cause a frameshift and a premature stop codon in exon 19, which would result in a truncated, or absent protein if subject to nonsense-mediated mRNA decay. We

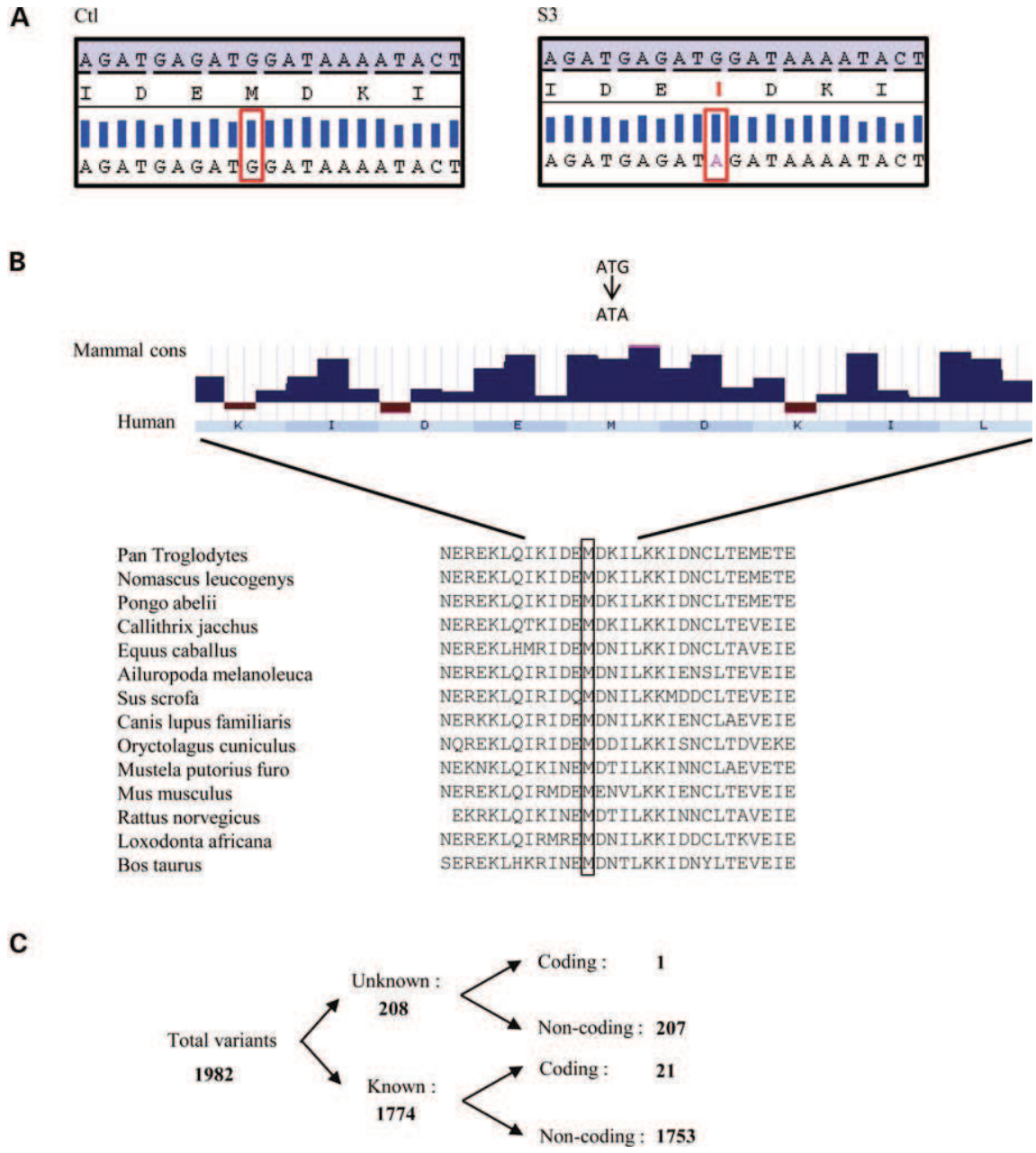

Figure 3. 2.7 Mb MCPH4 locus sequencing using 454 Roche GS FLX. (**A**) Sanger sequences of CASC5 exon 18 of proband (right) and control (left). (**B**) Amino acid sequence showing species conservation. (**C**) Compilation of variants observed by 454 FLX sequencing of the 2.7 Mb critical region.

used antibodies to detect a truncated or absent CASC5 protein in our patients affected with primary microcephaly. A CASC5 commercial antibody (Bethyl, catA300-805A) was first tested against human CASC5 from cell extracts (HEK293T, HELA and HTB10 human cell lines) and the endogenous protein was detectable at 265 kDa with higher expression in human embryonic kidney (Fig. 4C).

Western blots using whole cell lysates from patient's lymphoblastoid cell lines were performed. The endogenous protein was present in all subjects, including affected patients (Fig. 4D). In spite of intensive efforts using two commercials and non-commercial antibodies, including an antibody generously given by Kiyomitsu *et al*. (19), we failed to observe a clear and reproducible alteration in CASC5 protein expression in lymphoblastoid cell lines of affected subjects.

Cellular analyses

The *CASC5* knockdown in HeLa cells by siRNA causes a misalignment of chromosomes and premature entry into mitosis (19). We measured the growth rate of our patient's lymphoblast cells to determine whether the mitoses were more

Table 1. Table showing all coding variants found in our 2.7 Mb MCPH4 locus

Start Pos	End Pos	Ref bases	Var bases	Ref AA	Var AA	Region name	Known SNP Info db135
40 939 223	40939223	G	A	M	I	CASC5	
41 757 019	41757019	-	A	Q	T	RTF1	nc
41 672 634	41672634	A	G	*	*	NUSAP1	rs7168431
41 245 926	41245926	G	A	E	E	CHAC1	rs11557249
40 266 049	40266049	A	G	E	G	EIF2AK4	rs2307105
40 313 391	40313391	C	T	G	G	EIF2AK4	rs3207297
40 226 745	40226745	T	C	I	I	EIF2AK4	rs566792
40 330 814	40330814	C	T	K	K	SRP14	rs7321
41 829 480	41829480	A	G	L	L	RPAP1	rs721772
40 328 915	40328915	G	A	L	L	SRP14	rs8208
40 328 825	40328825	G	C	P	A	SRP14	rs7535
40 751 805	40751805	C	A	Q	K	BAHD1	rs3803357
41 815 766	41815766	G	C	Q	E	RPAP1	rs8027526
41 819 617	41819617	T	C	R	G	RPAP1	rs11630901
41 689 482	41689482	C	T	R	H	NDUFAF1	rs1899
41 689 416	41689416	C	A	R	L	NDUFAF1	rs3204853
41 813 529	41813529	C	T	R	R	RPAP1	rs3743031
40 583 810	40583810	G	T	R	R	PLCB2	rs62021888
41 106 176	41106176	T	G	S	A	ZFYVE19	rs690347
41 149 411	41149411	G	C	T	T	SPINT1	rs690458
41 476 715	41476715	G	A	T	T	EXD1	rs690733
41 634 837	41634838	AC	GA	T	D	NUSAP1	rs7178777
41 148 449	41148449	C	T	Y	Y	SPINT1	rs659232

Only one remains after ruling out a 454 FLX sequencing artifact not confirmed by Sanger sequencing (nc) (depth > 20, number of reads >90%).

frequent and/or abnormal, and searched for aneuploidies, which in turn can lead to apoptosis. Cell counting was performed every 48 h during 1 week and we compared lines from patients, unaffected family members and controls. However, the results showed no significant growth rate alteration (data not shown).

We also studied the cellular phenotype of our patients' lymphoblasts. Knocking down *CASC5* has been shown to produce micronuclei, a consequence of the misalignment of chromosomes during metaphase (19). No micronuclei were observed in our patients' fibroblasts when compared with controls (data not shown).

We used immunofluorescence (IF) to study the intracellular localization of CASC5, ZWINT-1, BUBR1, ASPM, CEP152 and PCTN during different phases of mitosis. Antibodies against these proteins were merged with an antibody recognizing alpha-tubulin, specific to the microtubules of the mitotic spindle (Fig. 5B). No specific defects were observed in fibroblasts of patients when compared with controls. Indeed, all proteins were correctly expressed and the mitotic spindles were normal, in our experimental setting.

DISCUSSION

We initially reported a linkage region (MCPH4) on chromosome 15 in a consanguineous family with primary microcephaly (18). Here, we re-analyzed this original family, and two other consanguineous families, using a genome-wide 250K GeneChip® SNP microarray. None of the families showed homozygosity at any known MCPH locus. One and only one region was found where the three families were homozygous over a significant length consistent with autozygosity (>2 cM in each family), a 3.7 Mb interval at 15q14–15.1. The three families originated from three small villages in rural Morocco before they immigrated to our country, consistent with a relatively recent common ancestor. The 3.7 Mb interval contained a 2.7 Mb-long haplotype that was shared by the three families (Fig. 1C), suggesting linkage disequilibrium around a common mutation. In the 2.7 Mb segment, we identified one rare coding mutation in *CASC5*, also known as *KNL1, Blinkin, AF15q14*, or *D40*. The mutation, c.6125 G>A, was absent from 316 unrelated control chromosomes (116 ethnically matched and 200 of various ethnicities), and was not observed among the 9500 alleles compiled by the Exome Variant Server (http://evs.gs.washington.edu/EVS/). The mutation was present in the three families, and segregated with primary microcephaly. Under the assumption of a mutation frequency of 0.003, the combined LOD score in the three families was >6. The genome-wide exclusion of other linkage regions, and the high LOD score, indicate that the MCPH-causing mutation lies within the 2.7 Mb interval.

CEP152 mutations have been reported as a cause of primary microcephaly within the 25 Mb MCPH4 locus that we initially reported (8). We excluded *CEP152* in the present families by three lines of evidence. First, no mutation was found by Sanger sequencing of the *CEP152* exons and flanking intronic sequences. Second, *CEP152* is located 7 Mb outside of the 3.7 Mb linkage region (Fig. 1C). Such a large distance is hardly compatible with the hypothesis of a mutation in the linkage interval acting as a distant regulator of *CEP152* gene expression (21), enhancers more distant than 1 Mb being exceptionally reported (22). Third, the *CEP152* protein was clearly present and normally expressed at the spindle poles in our patients' fibroblasts (Fig. 5B).

Sequencing *CASC5* in a cohort of patients with sporadic or familial primary microcephaly did not reveal any additional mutation, including three probands from consanguineous

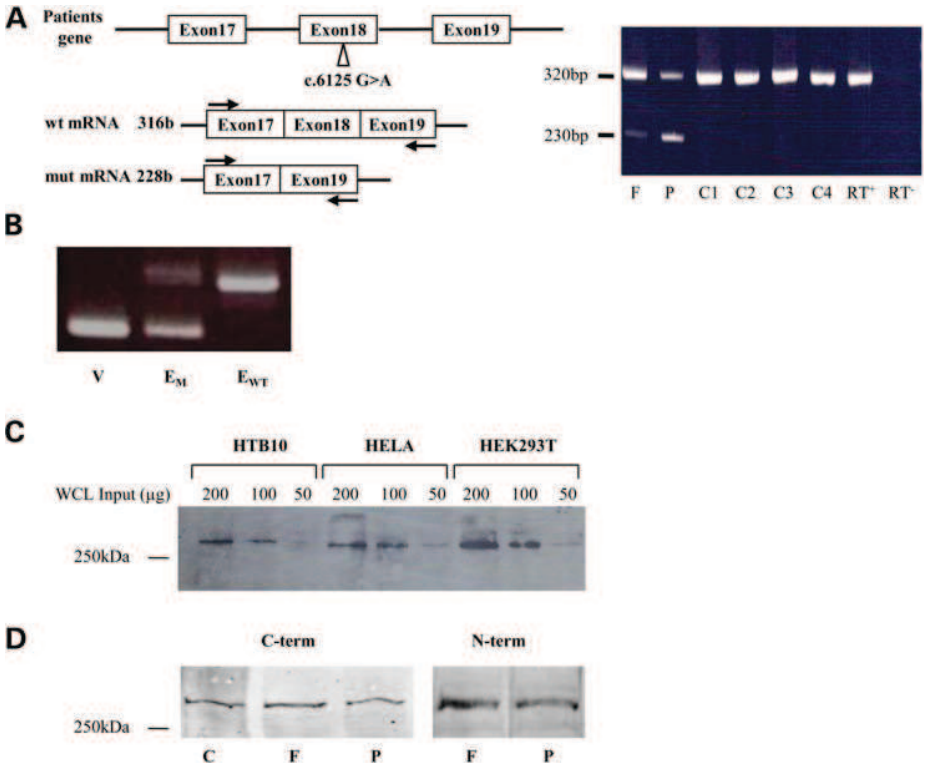

Figure 4. Functional effect of the mutation. (**A**) RT-PCR of random-primed RNA extracted from our patient's lymphoblastoïd cell lines. Amplified cDNAs using primers surrounding CASC5 exon 18 were loaded on 6% acrylamide gel. F: Unaffected father (family E); P: MCPH patient E3; C1-C4: unrelated normal controls; RT ±: positive and negative control of retrotranscription. Arrows indicate primers. A smaller band is observed in the homozygous patient and faintly in heterozygous father. Direct sequencing of this band extracted from the gel showed read-through from exon 17 into exon 19. Sequencing of the larger band at the expected size showed inclusion of exon 18 containing the mutation. (**B**) *Ex vivo* splicing assay for CASC5 variant. The cells were transfected with vectors containing two exons surrounding our exon of interest. One of the vectors contained the mutated exon 18 (EM), the other contained the wild-type exon 18 (EWT). Expressed mRNAs were detected on agarose gels. (**C**) Indicated amounts of whole cell lysates from HEK293T, HELA and HTB10 cells were separated on SDS-PAGE. CASC5 was detected by western blot using a commercial anti-CASC5 antibody. (**D**) Electrophoresis 100 µg of whole cell lysates from our patient's lymphoblastoïd cell lines, and western blotting detection of CASC5 using a polyclonal antibody against customized CASC5 peptides (C-term: left; N-term: right). F: Unaffected father (family E); P: MCPH patient E3.

families with homozygosity at the MCPH4 locus. We did not identify *CEP152* mutations in our cohort either, suggesting that both genes might be very rare causes of MCPH. Only four null mutations of *CASC5* are reported among 9500 alleles in the Exome Variant Server, suggesting a mutated allele frequency $<1/2000$ and a homozygote frequency $<1/4\,000\,000$ in an outbred population.

To further validate the *CASC5* mutation as the cause of MCPH in our patients, we sequenced the whole 2.7 Mb common homozygous haplotype by next generation sequencing. We used a customized hybridization array to capture the interval from our patients' DNA and sequenced the target-enriched DNA using a GS FLX 454 pyrosequencer. The *De novo* assembly of the sequencing reads showed no junction fragment that would have indicated an intra- or interchromosomal rearrangement. While this analysis produced 208 novel variants, only one unknown rare variant was observed in a protein-coding exon, c.6125 G>A. None of the noncoding variants affected a conserved noncoding element (23), and the critical interval did not contain an ultraconserved element (24). Although this analysis did not formally rule out a noncoding mutation with a functional effect, it supported the *CASC5* c.6125 mutation as the only coding and potentially highly penetrant mutation in our critical interval.

The transcriptome study focused on genes from the critical interval in lymphoblasts from two patients showed low signals for *CASC5* and normal signals for *CEP152*. Although these experiments are sensitive to cell culture conditions and we only had two patients' cell lines available for the study, these data provide some evidence for *CASC5* loss of function and for *CEP152* integrity.

Recently Fietz *et al*. analyzed the transcriptome of the germinal zone of the human fetal neocortex at 13–16 gestational weeks by RNA sequencing (25). They showed that the expression levels of *ASPM*, *CEP135* and *CASC5* were significantly upregulated in the human ventricular zone (VZ) compared with the subventricular zones (ISVZ and OSVZ) and cortical plate (CP) ($hVZ > hISVZ + hOSVZ + hCP$) and that the expression levels of *WDR62, CEP152, CENPJ*, *ASPM* and *CASC5* were down regulated in the CP compared with VZ and SVZs ($hCP < hVZ + hISVZ + hOSVZ$). These human fetal brain expression data identify *CASC5* as a gene which is upregulated in the VZ and downregulated in the CP, like *ASPM*, and are fully consistent with a CASC5 mutation affecting cell proliferation in the VZ, hence causing microcephaly.

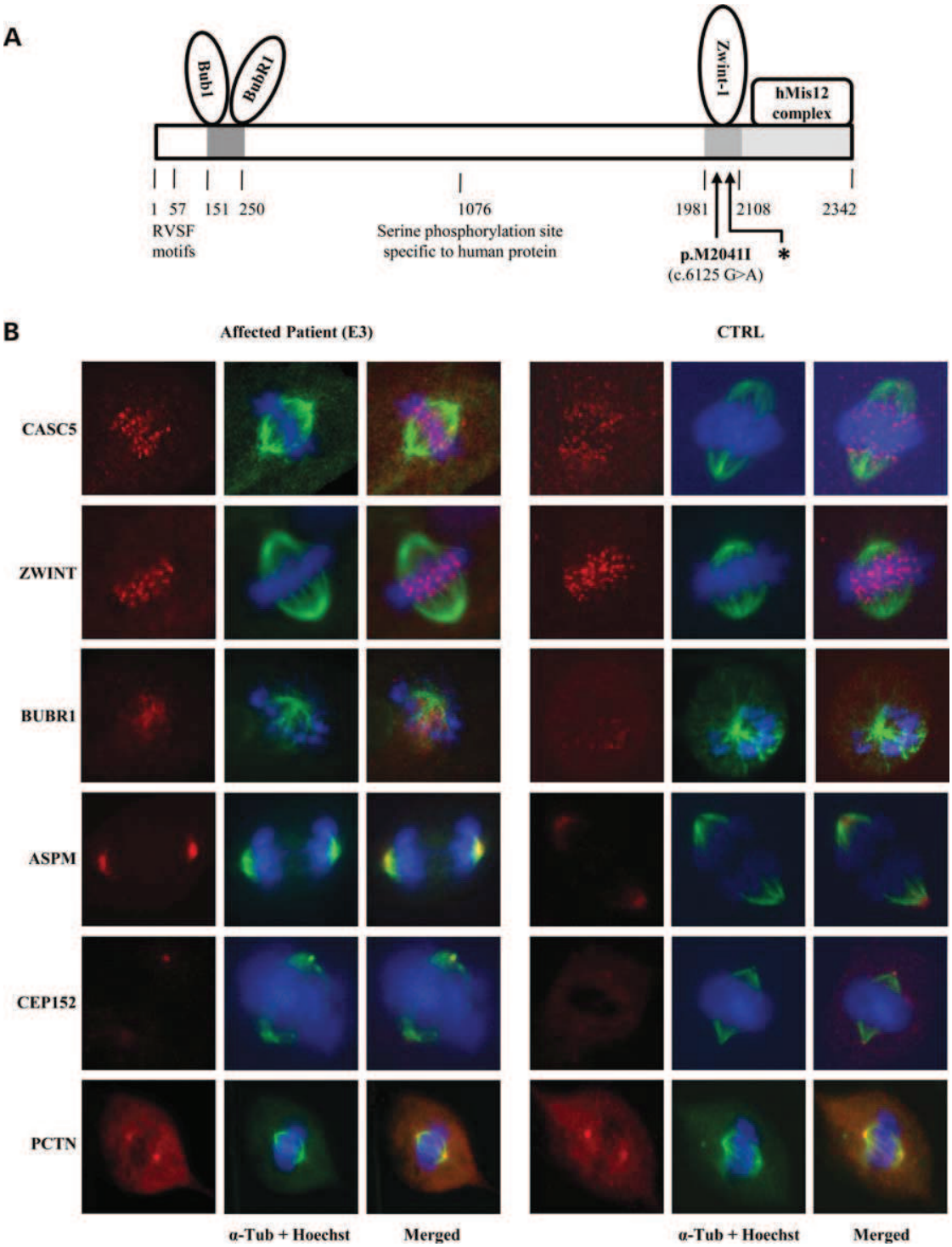

Figure 5. Mitotic morphology of our patients spindle in mitosis compared with control. (**A**) The longest isoform of protein CASC5 is made of 2342 amino acids encompassing 27 coding exons. The mutation found in our patients is indicated by the arrow. *stop codon in exon 19 induced by exon 18 skipping and subsequent frameshift. The areas of known interactions with partners are shown. (**B**) Immunofluorescence staining of fibroblasts carrying the M2041I mutation and control fibroblasts with antibodies against six proteins of interest (red, left column), α-tubulin (green, central column) and Hoechst (blue, central column) and the merged images (right column). The CASC5 antibody used in this experiment was the anti-Blinkin mouse monoclonal antibody 31F2 21. No specific defects observed.

CASC5 is a member of the conserved KMN (KNL1/Mis12 complex/Ndc80 complex) network of proteins which allows the docking of chromosome kinetochores to the microtubule apparatus. Correct docking is essential for adequate segregation of sister chromatids at anaphase, and is required for the spindle checkpoint of the mitotic cycle (19). CASC5

localization to the kinetochore is constant from G2 until late anaphase (26). Aurora Kinase B (AURKB) is a serine–threonine kinase that functions in the attachment of the mitotic spindle to the centromere during cell division for accurate chromosome segregation (27). A conserved motif in CASC5 directly interacts with and targets protein phosphatase 1 (PP1) to the outer kinetochore where it dephosphorylates AURKB substrates and stabilizes microtubule attachment. CASC5 thus opposes AURKB activity (28). Interestingly, CASC5 itself is a substrate for AURKB and phosphorylation of CASC5 by AURKB disrupts the CASC5-PP1 interaction (29). Moreover, the association of PP1 with the Spc7/Spc105/KNL1 family of kinetochore proteins is necessary to stabilize microtubule–kinetochore attachments and silence the SAC and the phospho-dependent recruitment of Bub1 and Bub3 to Spc7/KNL1 by Mph1 kinase maintains the spindle checkpoint (30).

The primate/rodent K_a/K_S analysis of *CASC5* shows a ratio of >1 (ratio $= 1.63$). This is very similar to other MCPH proteins *MCPH1*, *CDK5RAP2*, *ASPM* and *CENPJ*, strongly suggesting positive selection of *CASC5* in primate evolution leading to *Homo sapiens* and providing further evidence for *CASC5* as a MCPH gene. Of note, *CASC5* is part of the *ASPM* co-expression network in an exon-level study of the spatio-temporal transcriptome of the human brain (31).

CASC5 was recently identified as a protein presenting a human-specific phosphorylation site at serine 1076 that originated after the human–chimpanzee divergence (32). This might have a role in regulating CASC5 protein interaction networks in human cell division during brain development.

Analysis of the *CASC5* transcript in our patients' lymphoblasts, and of a mutated *CASC5* minigene *in vitro*, clearly showed that the exon 18 mutation causes exon skipping, which in turn produces a frameshift and a premature stop codon in exon 19 (Fig. 4A and B). The c.6125 G>A mutation is located in a portion of *CASC5* ranging from amino acid 1981 to 2108 known to specifically interact with ZWINT-1 (33). Downstream from the mutation, the C-terminus of CASC5 is essential for interacting with NSL1 and the MIS12 complex (34). Hence, the skipping of exon 18, frameshift and truncation induced by the mutation are expected to cause severe loss of *CASC5* function.

CASC5 binds to BUBR1 (also known as BUB1B) via an *N*-terminal domain, aa 151–250 (Fig. 5A) (35,36). A 2.2 Å resolution crystal structure of the complex has allowed detailed analysis of the binding interface between CASC5 and BUBR1, defining the stoichiometry and the affinity of the interaction (35). Kiyomitsu *et al*. described distinct and essential binding domains for BUB1 and BUBR1 at the N-terminus of CASC5 and for ZWINT-1 and hMis14/hNsl1 at the C-terminus of the protein (33). BUB1B loss of function in man causes Mosaic Variegated Aneuploidy (MVA) Syndrome 1 (MIM 257300), an autosomal recessive microcephaly phenotype linked to a mitotic chromosomal segregation defect leading to aneuploidy for various chromosomes in fractions of cells in many tissues (37). It is hence reasonable to speculate that primary microcephaly in both *CASC5* and *BUBR1* defects results from a common mechanism involving chromosome missegregation.

CASC5 protein was present in lymphoblasts of our patients with a homozygous mutation. Furthermore, in contrast with MVA or other syndromes with microcephaly like the *PCNT* defect (38), our lymphoblasts morphological studies did not detect aneuploidy, abnormal mitoses or other nuclear anomalies. We speculate that only some tissues, including neural cell progenitors, fully express the defect and would show a truncated, or absent, CASC5 protein. The normal phenotype in the non-neurological cells we studied is consistent with the absence of leukemia or tumors in our patients, which contrasts with cancer-proneness in MVA.

The *CASC5* knockdown in HeLa cells by siRNA causes a misalignment of chromosomes and premature entry into mitosis (19). Premature entry into mitosis is also observed in MCPH caused by the *microcephalin* (*MCPH1*) defect, where it is thought to cause microcephaly by its critical role in neural progenitors. In the latter cells, coupling of the mitosis and centrosome cycles is required for proper symmetric versus asymmetric division and hence for appropriate proliferation, which in turn will result in an appropriate number of neurons and a normal-sized brain (16). MCPH1 patients' cells show premature chromosome condensation (39) and abnormal chromosome alignment is observed in a mouse MCPH1 model (16). Our *CASC5*-mutated patients' lymphoblasts did not display premature chromosome condensation or nuclear features associated with the *CASC5* knockdown, e.g. micronuclei. Our results may reflect normality of the *CASC5* function in the cell types we tested, i.e. fibroblasts and lymphoblasts from our patients, and/or functional redundancy in these cells, as opposed to our patients' neural progenitor cells. Indeed, mRNA and protein analyses in lymphoblasts showed the presence of some normally spliced transcript (Fig. 4A) and the presence of a normal-sized protein. Inducing pluripotent stem cells from our patients' fibroblasts and deriving them *in vitro* into the brain cortex (40) may eventually answer this question.

In conclusion, we identified a rare mutation of the kinetochore KMN network gene *CASC5* in three families with autosomal recessive primary microcephaly (MCPH). We provide evidence that the mutation disrupts *CASC5* function, and show features of accelerated evolution of *CASC5* in the *Homo sapiens* lineage. *CASC5* is upregulated in the VZ of the human fetal brain, it is required for the spindle checkpoint of the mitotic cycle and its knockdown causes premature entry into mitosis. Our data provide strong evidence for *CASC5* as a novel microcephaly gene, underscoring the role of the kinetochore in proper volumetric development of the human brain.

MATERIALS AND METHODS

Patients and families

Family E has been reported previously (18). Two consanguineous families S and Y from Morocco with three and one affected children, respectively, were later referred to us for primary microcephaly. The three families were unaware of common ancestry but originate from three villages <50 km apart in rural Morocco. All patients have HC -4 to -7 SD relative to the mean for age and gender, and all have

congenital microcephaly except S2, whose HC at birth was reported at fifth centile (Fig. 1A–C). All patients have a normal stature and reached motor milestones within the normal time limits. None had epilepsy or neurological deficits. No additional malformation was reported and medical histories are unremarkable. The oldest patients are now older than 30 years with no history of leukemia or tumors. All have mild-to-moderate mental retardation.

Homozygosity mapping and Sanger sequencing

DNAs from index patients from the three families were genotyped using 250K SNP GeneChip® microarrays (Affymetrix™, Inc.) following manufacturer's instructions. Homozygous stretches were delineated using the HomozygosityMapper software (41).

Prioritization of candidate genes

K_a/K_s is the ratio between the rate of nonsynonymous mutations and the rate of synonymous mutations observed in a gene by comparing two species. The ratio enables to measure the rate at which the gene product has changed in terms of amino acids, in comparison with what is expected in the case of random mutations (neutral evolution). A ratio >1 is a sign of positive selection (42). Protein sequences were compared between human and macaque and between mouse and rat. K_a = standardized ratio of nonsynonymous mutations in the protein, K_s = standardized ratio of synonymous mutations, occurring in the degenerate positions of codon.

Endeavor (www.esat.kuleuven.be/endeavour) was used to rank all the genes located in our linkage interval using publicly available data regarding genes known to cause other forms of microcephaly and/or to locate at the centrosome.

Transcriptome study

Five micrograms of RNA were purified using the RNeasy mini kit (Qiagen) from E3, S1 and one unrelated control. They were hybridized to an Affymetrix® GeneChip Human Genome U133 Plus 2.0 Array. Experiments and analyses were performed following manufacturer's instructions.

Sanger sequencing

PCR primers for all candidate genes were designed using the Exonprimer software. 'Touchdown' PCR products were loaded on agarose gels. The coding regions and exon–intron junctions of the candidate genes were sequenced using the Big Dye Terminator cycle sequencing kit v2 (Applied Biosystems, Foster City, CA, USA), and analyzed on a 3130 Genetic Analyzer sequencing machine (Applied Biosystems). Sequences were inspected *in silico* for mutations using the SeqScape software V.2.0. (Applied Biosystems).

Next generation sequencing of the critical region

A 2.7 Mb genomic segment corresponding to the critical linkage region of the MCPH4 locus was captured from a sonicated sample of 21 μg purified genomic DNA of E1, E2, E3, S1 and S3 on the solid phase using a customized Sequence Capture 385K Human Array, designed and manufactured by Roche NimbleGen. A total of 385 000 unique, non-tiling probes 60–90 nucleotides in length were designed to encompass the whole critical region (chromosome 15: 36,948,439-39,645,979; NCBI build 36, hg18), excluding repetitive DNA. The target region-enriched DNA was then sequenced using a GS-FLX 454 pyrosequencer. Emulsion PCR and pyrosequencing were performed in a PicoTiter Plate as described in the GS-FLX Titanium sequencing manual. Sequencing data were filtered for changes present in $<10\%$ of reads or in fewer than two reads. The filtered data were analyzed using the following software: GS *De Novo* Assembler (which allows for the detection of junction fragments in chromosomal translocations or inversions), GS Reference Mapper (which compares the sequence of interest with the reference sequence and identifies small insertions or deletions, and SNPs) and GS Amplicon Variant Analyzer (which identifies unknown variants and their respective frequencies in large data pool).

Cell culture

Lymphoblastoïd cell lines were cultured in Roswell Park Memorial Institute medium 1640 (Invitrogen) supplemented with 10% fetal bovine serum (Invitrogen), 100 U/ml penicillin (Invitrogen), 100 μg/ml streptomycin (Invitrogen), 2.5 μg/ml fungizone (Invitrogen) and 2 mM L-glutamine (Invitrogen). Fibroblasts were cultured in Dulbecco's modified Eagle's medium (Invitrogen) supplemented with 10% fetal bovine serum (Invitrogen), 100 U/ml penicillin (Invitrogen), 100 μg/ml streptomycin (Invitrogen), 2.5 μg/ml fungizone (Invitrogen) and 2 mM Na pyruvate (Invitrogen). Cells were grown at 37°C in a 5% CO2-humidified atmosphere.

RNA extraction and RT-PCR

Lymphoblastoïd cell lines were lysed in Tri-reagent (Ambion) and centrifuged for 10 min at 13 000 rpm at 4°C. Two hundred microliters of RNase-free chloroform (VWR Prolabo) were added to the supernatant. Each sample was then centrifuged at 15 000*g* for 15 min at 4°C. One volume of ice cold 70% ethanol was then added to the supernatant. Each sample was then purified on RNeasy columns (Qiagen) according to the manufacturer's instructions. Once purified, 2.5 μl of the RNA samples was subjected to reverse transcription using the Super-Script II Reverse Transcriptase kit (Invitrogen) following the manual instructions. Once all the samples were reverse transcribed, 50 ng of template cDNA was engaged in a 'touchdown' PCR: initial denaturation at 94°C for 2.5 min, 20 cycles including denaturation at 94°C, hybridization at 62°C–52°C (−0.5°C each cycle) and elongation at 72°C, followed by 20 other cycles at a constant 52°C melting temperature. The primers used for *CASC5* cDNA amplification were: 5′-TCTGACAAAGAGCTGAAGGC-3′ and 5′-CTTAACCT TGTCGACTTTTGA-3′. PCR products were then loaded on 6% tris, borate, EDTA (TBE) acrylamide gel (Invitrogen) during 1 h at 110 V in TBE buffer.

Minigene construction and expression

CASC5 exon 18 was amplified by PCR, with 150 bp of 5′ and 3′ flanking intronic sequences, using forward and reverse primers carrying 5′ tails containing appropriate restriction sites, and inserted into the BamHI and MluI restriction sites of the pCAS-1 vector (43). Minigenes carrying the wild-type or the variant allele were then identified by direct sequencing and were transfected separately into HeLa cells in the same

experiment. RNA was extracted from transfected cells and the splicing patterns corresponding to the wild-type and mutant alleles were then compared by RT-PCR analysis, using universal primers in the exons of the pCAS minigene and by sequencing all RT-PCR products.

Antibodies

Anti-*CASC5* rabbit polyclonal antibody (Bethyl, catA300-805A; Abcam, ab70537), Anti-*Blinkin* mouse monoclonal antibody 31F2 (19), anti-*ZWINT-1* rabbit polyclonal antibody (Abcam, ab84367), anti-*BUBR1* mouse monoclonal antibody (Abcam, ab54894), anti-*ASPM* rabbit polyclonal antibody (Bethyl, catIHC-00058), anti-*CEP152* rabbit polyclonal antibody (Bethyl, catA302-480A), anti-*PCTN* rabbit polyclonal antibody (Covance, pRb-432C) and anti-α-*TUBULIN* mouse polyclonal (Sigma,T6793) were obtained commercially. Polyclonal Antibodies against costumed peptides of *CASC5* protein were produced by Eurogentec (https ://secure.eurogentec.com/product/research-double-peptide-a nti-peptide-polyclonal-packages.html). N-terminal peptide: (AA 1–15) MDGVSSEANEENDNI and C-terminal peptide: (AA 2036-2050) IKIDEMDKILKKIDN.

Immunoblotting

Lymphoblastoïd cell lines were washed twice with ice cold phosphate-buffered saline (PBS) and harvested with lysis buffer [50 mM Tris HCl pH 8, 150 mM NaCl, 1% NP-40, 0.5% sodium deoxycholate 0.1% sodium dodecyl sulfate (SDS), 4 mM sodium orthovanadate, 5 mM Na4P2O7, 1 μM okadaic acid and a mix of protease inhibitors Complete (Roche Diagnostics)] for 60 min at 4°C. The cell lysates were clarified by centrifugation at 15 000*g* for 10 min at 4°C and the protein concentration was measured using the Bradford assay. Different quantities of the whole cell lysate were separated by sodium dodecyl sulfate-polyacrylamide gel electrophoresis (SDS-PAGE), transferred onto nitrocellulose membranes and immunoblotted using appropriate antibodies. Proteins of interest were then revealed using ECL (enhanced chemiluminescence) kits (PerkinElmer) or using an Odyssey Infrared Imaging System (LI-COR Biosciences).

Immunofluorescence

Fibroblasts were seeded on coverslips in 12-well plates at 5×10^4 cells per well in the supplemented Dulbecco's modified Eagle's medium as described above. Forty-eight hours after seeding, the cells were washed twice with PBS, fixed with 4% paraformaldehyde (PFA 4%) for 30 min at room temperature or methanol for 10 min at −20°C and washed again twice with PBS. The cells were then incubated with blocking/permeabilization solution for 30 min, with the primary antibody solution for 2 h, washed three times with PBS and incubated with the secondary antibody for an hour preserved from light. Coverslips were then washed three times with PBS, incubated with Hoechst 33342 (Invitrogen), washed three times with PBS and fixed with Fluorsafe (Calbiochem). Finally, IF was analyzed using a Zeiss Axioplan 2 Imaging microscope.

ACKNOWLEDGEMENTS

We thank C. Sotiriou (J Bordet Institute, Brussels) for transcriptome arrays, J. Van Durme for implementing the K_a/K_s software, P. Vanderhaeghen for interesting discussions, and Z. Ajarchouh, S. Strollo and C. Degraef for expert technical help. We thank T. Kiyomiysu for generous gift of the 31F2 antibody. We thank the patients and families for participating in the study.

Conflict of Interest statement. None declared.

FUNDING

M.A. was supported by the Fonds de la Recherche Scientifique Medicale (FRSM) of the Belgian FNRS and by the Fonds Erasme. A.G. was supported by the Fonds pour la formation à la Recherche dans l'Industrie et dans l'Agriculture (FRIA) and by the Fonds David et Alice Van Buuren. N.L. is a clinician-scientist of the FNRS.

REFERENCES

1. Barkovich, A.J., Guerrini, R., Kuzniecky, R.I., Jackson, G.D. and Dobyns, W.B. (2012) A developmental and genetic classification for malformations of cortical development: update 2012. *Brain*, **135**, 1348–1369.
2. Bond, J., Roberts, E., Mochida, G.H., Hampshire, D.J., Scott, S., Askham, J.M., Springell, K., Mahadevan, M., Crow, Y.J., Markham, A.F. *et al.* (2002) ASPM is a major determinant of cerebral cortical size. *Nat. Genet.*, **32**, 316–320.
3. Tolmie, J.L., McNay, M., Stephenson, J.B., Doyle, D. and Connor, J.M. (1987) Microcephaly: genetic counselling and antenatal diagnosis after the birth of an affected child. *Am. J. Med. Genet.*, **27**, 583–594.
4. Woods, C.G., Bond, J. and Enard, W. (2005) Autosomal recessive primary microcephaly (MCPH): a review of clinical, molecular, and evolutionary findings. *Am. J. Hum. Genet.*, **76**, 717–728.
5. Jackson, A.P., Eastwood, H., Bell, S.M., Adu, J., Toomes, C., Carr, I.M., Roberts, E., Hampshire, D.J., Crow, Y.J., Mighell, A.J. *et al.* (2002) Identification of microcephalin, a protein implicated in determining the size of the human brain. *Am. J. Hum. Genet.*, **71**, 136–142.
6. Nicholas, A.K., Khurshid, M., Desir, J., Carvalho, O.P., Cox, J.J., Thornton, G., Kausar, R., Ansar, M., Ahmad, W., Verloes, A. *et al.* (2010) WDR62 is associated with the spindle pole and is mutated in human microcephaly. *Nat. Genet.*, **42**, 1010–1014.
7. Bond, J., Roberts, E., Springell, K., Lizarraga, S.B., Scott, S., Higgins, J., Hampshire, D.J., Morrison, E.E., Leal, G.F., Silva, E.O. *et al.* (2005) A centrosomal mechanism involving CDK5RAP2 and CENPJ controls brain size. *Nat. Genet.*, **37**, 353–355.
8. Guernsey, D.L., Jiang, H., Hussin, J., Arnold, M., Bouyakdan, K., Perry, S., Babineau-Sturk, T., Beis, J., Dumas, N., Evans, S.C. *et al.* (2010) Mutations in centrosomal protein CEP152 in primary microcephaly families linked to MCPH4. *Am. J. Hum. Genet.*, **87**, 40–51.
9. Kumar, A., Girimaji, S.C., Duvvari, M.R. and Blanton, S.H. (2009) Mutations in STIL, encoding a pericentriolar and centrosomal protein, cause primary microcephaly. *Am. J. Hum. Genet.*, **84**, 286–290.
10. Sir, J.H., Barr, A.R., Nicholas, A.K., Carvalho, O.P., Khurshid, M., Sossick, A., Reichelt, S., D'Santos, C., Woods, C.G. and Gergely, F. (2011) A primary microcephaly protein complex forms a ring around parental centrioles. *Nat. Genet.*, **43**, 1147–1153.
11. Hussain, M.S., Baig, S.M., Neumann, S., Nurnberg, G., Farooq, M., Ahmad, I., Alef, T., Hennies, H.C., Technau, M., Altmuller, J. *et al.* (2012) A Truncating Mutation of CEP135 Causes Primary Microcephaly and Disturbed Centrosomal Function. *Am. J. Hum. Genet.*, **90**, 871–878.
12. Marchal, J.A., Ghani, M., Schindler, D., Gavvovidis, I., Winkler, T., Esquitino, V., Sternberg, N., Busche, A., Krawitz, P., Hecht, J. *et al.* (2011) Misregulation of mitotic chromosome segregation in a new type of autosomal recessive primary microcephaly. *Cell Cycle*, **10**, 2967–2977.

13. Zhong, X., Liu, L., Zhao, A., Pfeifer, G.P. and Xu, X. (2005) The abnormal spindle-like, microcephaly-associated (ASPM) gene encodes a centrosomal protein. *Cell Cycle*, **4**, 1227–1229.
14. Zhong, X., Pfeifer, G.P. and Xu, X. (2006) Microcephalin encodes a centrosomal protein. *Cell Cycle*, **5**, 457–458.
15. Fish, J.L., Kosodo, Y., Enard, W., Paabo, S. and Huttner, W.B. (2006) Aspm specifically maintains symmetric proliferative divisions of neuroepithelial cells. *Proc. Natl Acad. Sci. USA*, **103**, 10438–10443.
16. Gruber, R., Zhou, Z., Sukchev, M., Joerss, T., Frappart, P.O. and Wang, Z.Q. (2011) MCPH1 regulates the neuroprogenitor division mode by coupling the centrosomal cycle with mitotic entry through the Chk1-Cdc25 pathway. *Nat. Cell Biol.*, **13**, 1325–1334.
17. Peng, G., Yim, E.K., Dai, H., Jackson, A.P., Burgt, I., Pan, M.R., Hu, R., Li, K. and Lin, S.Y. (2009) BRIT1/MCPH1 links chromatin remodelling to DNA damage response. *Nat. Cell Biol.*, **11**, 865–872.
18. Jamieson, C.R., Govaerts, C. and Abramowicz, M.J. (1999) Primary autosomal recessive microcephaly: homozygosity mapping of MCPH4 to chromosome 15. *Am. J. Hum. Genet.*, **65**, 1465–1469.
19. Kiyomitsu, T., Obuse, C. and Yanagida, M. (2007) Human Blinkin/AF15q14 is required for chromosome alignment and the mitotic checkpoint through direct interaction with Bub1 and BubR1. *Dev. Cell*, **13**, 663–676.
20. Kline, S.L., Cheeseman, I.M., Hori, T., Fukagawa, T. and Desai, A. (2006) The human Mis12 complex is required for kinetochore assembly and proper chromosome segregation. *J. Cell Biol.*, **173**, 9–17.
21. Krivega, I. and Dean, A. (2011) Enhancer and promoter interactions-long distance calls. *Curr. Opin. Genet. Dev.*, **22**, 79–85.
22. Volkmann, B.A., Zinkevich, N.S., Mustonen, A., Schilter, K.F., Bosenko, D.V., Reis, L.M., Broeckel, U., Link, B.A. and Semina, E.V. (2011) Potential novel mechanism for Axenfeld-Rieger syndrome: deletion of a distant region containing regulatory elements of PITX2. *Invest. Ophthalmol. Vis. Sci.*, **52**, 1450–1459.
23. Halligan, D.L., Oliver, F., Guthrie, J., Stemshorn, K.C., Harr, B. and Keightley, P.D. (2011) Positive and negative selection in murine ultraconserved noncoding elements. *Mol. Biol. Evol.*, **28**, 2651–2660.
24. Bejerano, G., Pheasant, M., Makunin, I., Stephen, S., Kent, W.J., Mattick, J.S. and Haussler, D. (2004) Ultraconserved elements in the human genome. *Science*, **304**, 1321–1325.
25. Fietz, S.A., Lachmann, R., Brandl, H., Kircher, M., Samusik, N., Schroder, R., Lakshmanaperumal, N., Henry, I., Vogt, J., Riehn, A. *et al.* (2012) Transcriptomes of germinal zones of human and mouse fetal neocortex suggest a role of extracellular matrix in progenitor self-renewal. *Proc. Natl Acad. Sci. USA*, **109**, 11836–11841.
26. Cheeseman, I.M., Hori, T., Fukagawa, T. and Desai, A. (2008) KNL1 and the CENP-H/I/K complex coordinately direct kinetochore assembly in vertebrates. *Mol. Biol. Cell*, **19**, 587–594.
27. Lampson, M.A. and Kapoor, T.M. (2005) The human mitotic checkpoint protein BubR1 regulates chromosome-spindle attachments. *Nat. Cell Biol.*, **7**, 93–98.
28. Liu, D., Vleugel, M., Backer, C.B., Hori, T., Fukagawa, T., Cheeseman, I.M. and Lampson, M.A. (2010) Regulated targeting of protein phosphatase 1 to the outer kinetochore by KNL1 opposes Aurora B kinase. *J. Cell Biol.*, **188**, 809–820.
29. Welburn, J.P., Vleugel, M., Liu, D., Yates, J.R. III, Lampson, M.A., Fukagawa, T. and Cheeseman, I.M. (2010) Aurora B phosphorylates spatially distinct targets to differentially regulate the kinetochore-microtubule interface. *Mol. Cell*, **38**, 383–392.
30. Shepperd, L.A., Meadows, J.C., Sochaj, A.M., Lancaster, T.C., Zou, J., Buttrick, G.J., Rappsilber, J., Hardwick, K.G. and Millar, J.B. (2012) Phosphodependent recruitment of Bub1 and Bub3 to Spc7/KNL1 by Mph1 kinase maintains the spindle checkpoint. *Curr. Biol.*, **22**, 891–899.
31. Kang, H.J., Kawasawa, Y.I., Cheng, F., Zhu, Y., Xu, X., Li, M., Sousa, A.M., Pletikos, M., Meyer, K.A., Sedmak, G. *et al.* (2011) Spatio-temporal transcriptome of the human brain. *Nature*, **478**, 483–489.
32. Kim, D.S. and Hahn, Y. (2011) Identification of novel phosphorylation modification sites in human proteins that originated after the human–chimpanzee divergence. *Bioinformatics*, **27**, 2494–2501.
33. Kiyomitsu, T., Murakami, H. and Yanagida, M. (2011) Protein interaction domain mapping of human kinetochore protein Blinkin reveals a consensus motif for binding of spindle assembly checkpoint proteins Bub1 and BubR1. *Mol. Cell Biol.*, **31**, 998–1011.
34. Petrovic, A., Pasqualato, S., Dube, P., Krenn, V., Santaguida, S., Cittaro, D., Monzani, S., Massimiliano, L., Keller, J., Tarricone, A. *et al.* (2010) The MIS12 complex is a protein interaction hub for outer kinetochore assembly. *J. Cell Biol.*, **190**, 835–852.
35. Bolanos-Garcia, V.M., Lischetti, T., Matak-Vinkovic, D., Cota, E., Simpson, P.J., Chirgadze, D.Y., Spring, D.R., Robinson, C.V., Nilsson, J. and Blundell, T.L. (2011) Structure of a Blinkin-BUBR1 complex reveals an interaction crucial for kinetochore-mitotic checkpoint regulation via an unanticipated binding Site. *Structure*, **19**, 1691–1700.
36. Krenn, V., Wehenkel, A., Li, X., Santaguida, S. and Musacchio, A. (2012) Structural analysis reveals features of the spindle checkpoint kinase Bub1-kinetochore subunit Knl1 interaction. *J. Cell Biol.*, **196**, 451–467.
37. Hanks, S., Coleman, K., Reid, S., Plaja, A., Firth, H., Fitzpatrick, D., Kidd, A., Mehes, K., Nash, R., Robin, N. *et al.* (2004) Constitutional aneuploidy and cancer predisposition caused by biallelic mutations in BUB1B. *Nat. Genet.*, **36**, 1159–1161.
38. Rauch, A., Thiel, C.T., Schindler, D., Wick, U., Crow, Y.J., Ekici, A.B., van Essen, A.J., Goecke, T.O., Al-Gazali, L., Chrzanowska, K.H. *et al.* (2008) Mutations in the pericentrin (PCNT) gene cause primordial dwarfism. *Science*, **319**, 816–819.
39. Neitzel, H., Neumann, L.M., Schindler, D., Wirges, A., Tonnies, H., Trimborn, M., Krebsova, A., Richter, R. and Sperling, K. (2002) Premature chromosome condensation in humans associated with microcephaly and mental retardation: a novel autosomal recessive condition. *Am. J. Hum. Genet.*, **70**, 1015–1022.
40. Gaspard, N., Bouschet, T., Hourez, R., Dimidschstein, J., Naeije, G., van den Ameele, J., Espuny-Camacho, I., Herpoel, A., Passante, L., Schiffmann, S.N. *et al.* (2008) An intrinsic mechanism of corticogenesis from embryonic stem cells. *Nature*, **455**, 351–357.
41. Seelow, D., Schuelke, M., Hildebrandt, F. and Nurnberg, P. (2009) HomozygosityMapper––an interactive approach to homozygosity mapping. *Nucleic Acids Res.*, **37**, W593–W599.
42. Dorus, S., Vallender, E.J., Evans, P.D., Anderson, J.R., Gilbert, S.L., Mahowald, M., Wyckoff, G.J., Malcom, C.M. and Lahn, B.T. (2004) Accelerated evolution of nervous system genes in the origin of Homo sapiens. *Cell*, **119**, 1027–1040.
43. Gaildrat, P., Killian, A., Martins, A., Tournier, I., Frebourg, T. and Tosi, M. (2010) Use of splicing reporter minigene assay to evaluate the effect on splicing of unclassified genetic variants. *Methods Mol. Biol.*, **653**, 249–257.